

Slow nanoscale dynamics of ionic liquids below the glass transition observed by low radiation dose XPCS

Jan Verwohlt¹, Mario Reiser^{1,2}, Lisa Randolph¹, Aleksandar Matic³, Luis Aguilera Medina³, Anders Madsen², Michael Sprung⁴, Alexey Zozulya^{2,4} and Christian Gutt^{1*}

¹ Department Physik, Universität Siegen, D-57072 Siegen, Germany

² European X-Ray Free-Electron Laser Facility, 22869 Schenefeld, Germany

³ Department of Physics, Chalmers University of Technology, 41258 Gothenburg, Sweden

⁴ Deutsches Elektronen-Synchrotron DESY, Hamburg, Germany

* gutt@physik.uni-siegen.de

Abstract

X-ray radiation damage provides a serious bottle neck for investigating μs to s dynamics on nanometer length scales employing X-ray photon correlation spectroscopy. This limitation hinders the investigation of real time dynamics in most soft matter and biological materials which can tolerate only X-ray doses of kGy and below. Here, we show that this bottleneck can be overcome by low dose X-ray speckle visibility spectroscopy. Employing X-ray doses of 640 Gy to 8 kGy and analyzing the sparse speckle pattern of count rates of 10^{-2} per pixel and below we follow the slow nanoscale dynamics of an ionic liquid (IL) at the glass transition. At the pre-peak of nanoscale order in the IL we observe complex dynamics upon approaching the glass transition temperature T_G with a freezing in of the alpha relaxation and a multitude of milli-second local relaxations existing well below T_G . We identify this fast relaxation as being responsible for the increasing development of nanoscale order observed in ILs at temperatures below T_G .

Introduction

The glass transition of a supercooled liquid is characterized by a dramatic slowing down of its dynamics with the atomic and nanoscale relaxation reaching time scales of seconds or even slower. Measuring such slow dynamics on the nano- or atomic scale is a considerable experimental challenge. It can be addressed directly by X-ray photon correlation spectroscopy (XPCS) experiments employing coherent X-ray beams[1-7] by tracing fluctuations in X-ray speckle patterns. However, the highly intense X-ray beams of 3rd generation storage rings can also be the cause of considerable radiation damage to the samples. Atomic scale XPCS experiments use X-ray doses of MGy and beyond which can lead to beam induced dynamics even in hard condensed matter samples [8]. Soft and biological matter samples are much more sensitive to radiation damage rendering XPCS experiments with MGy X-ray doses impossible. To overcome this bottle neck of radiation damage is even more important for the upcoming diffraction limited storage rings (DLSR) which provide an increase in X-ray brilliance of up to two orders of magnitude [2,9,10]. The remedy for beam damage is frequent sample replacement as can be realized using e.g. flow cells or changing the exposure spot on the sample. However, low dose XPCS experiments often show very noisy correlation functions

which do not yield conclusive insights into the dynamics or did not extend beyond feasibility studies [11,12].

Here, we demonstrate that XPCS experiments can be performed with low noise levels at radiation doses ranging from a few 1000 Gy down to the sub 700 Gy regime. The concept consists in spreading the dose needed for a correlation function over the entire sample volume by measuring at every spot on the sample the visibility of a speckle pattern as a function of exposure time. Mitigating the absorbed dose in this way is done at the expense of signal strength; the collected speckle patterns are sparse containing less than 10^{-2} photons per pixel. We show that the correlation function can nevertheless be extracted by proper assignment of photon probabilities using a sufficiently large number of images.

Ionic liquids (ILs) are molten salts which show a structural heterogeneity on the nanoscale [13,14]. This nanoscale segregation or domain formation is evidenced by a characteristic pre-peak in diffraction experiments at Q-positions around $Q=2-3 \text{ nm}^{-1}$, much smaller than the molecular structure factor. The intensity of this pre-peak increases with decreasing temperature with the intriguing finding that it does not saturate at T_G but instead this nanoscale correlation is found to increase even at temperatures well below T_G [15]. Neutron spin echo (NSE) experiments revealed that this pre-peak is accompanied by complex heterogeneous dynamics with multiple relaxation channels in the picosecond to nanosecond regime at temperatures well above T_G [15]. However, the dynamics at and below the glass transition is occurring on time scales too slow for NSE experiments and has thus so far not been investigated. Applying our scheme, we are able to investigate the nanoscale dynamics of an imidazolium-based ionic liquid (C8mimCl, $C_{12}H_{23}ClN_2$) around its glass transition temperature.

The self-assembled nanoscale order of the ionic liquids is based upon a delicate balance between electrostatic and van-der Waals forces and thus very sensitive to radiation damage. This order quickly decays under the highly intense coherent X-ray beam of 3rd generation storage rings making a traditional XPCS experiment based on collecting long series of speckle patterns for determining the intensity autocorrelation function not feasible.

Theory of low intensity X-ray speckle visibility spectroscopy

XPCS experiments extract from a time series of fluctuating X-ray speckle patterns the intensity autocorrelation function

$$g_2(Q, \tau) = \langle I(Q, t)I(Q, t + \tau) \rangle / \langle I(Q, t) \rangle^2, \text{ Eq. (1)}$$

with τ denoting the time delay between two frames of the recorded time series. The intensity autocorrelation function is directly linked to the intermediate scattering function (ISF) $f(Q, \tau)$ via the Siegert relation

$$g_2(Q, \tau) = 1 + \beta(Q)|f(Q, \tau)|^2 \quad \text{Eq. (2)}$$

with $\beta(Q)$ the (Q-dependent) X-ray speckle contrast. Exposure to the beam can be minimized by measuring at each sample position only two speckle patterns with an adjustable time delay τ between them [16,17]. Faster dynamics can be measured by adjustable exposure times t_e

on each sample position and analyzing the contrast of single smeared out speckle patterns as a function of exposure time t_e (X-ray speckle visibility spectroscopy). In this case the speckle contrast is given by [18]

$$\beta(Q, t_e) = \frac{\beta_0}{t_e} \int_0^{t_e} 2 \left(1 - \frac{t}{t_e}\right) |f(Q, \tau)|^2 d\tau \quad \text{Eq. (3)}$$

which yields access to the ISF.

The requirement of tracing ms dynamics and low radiation doses results in speckle patterns of very low intensities on the order of 10^{-2} photons/pixel and below. The probability of detecting k photons during an exposure time t_e is given by the negative binominal distribution (NBD) [19]

$$P(k, t_e) = \frac{\Gamma(k+M(t_e))}{\Gamma(M(t_e))\Gamma(k+1)} \left(1 + \frac{M(t_e)}{\bar{k}}\right)^{-k} \left(1 + \frac{\bar{k}}{M(t_e)}\right)^{-M(t_e)}. \quad \text{Eq. (4)}$$

The average photon probability \bar{k} is given by n_{ph}/n_{pix} with n_{ph} denoting the total number of photons on the detector and n_{pix} the number of pixels. The number of modes in a single speckle pattern is $M(t_e) = M_t \cdot M_l \cdot M_{dyn}(t_e)$ where M_t is the number of transverse modes and M_l the number of longitudinal modes. Both values are fixed and depend on the degree of coherence of the X-ray beam and the geometry of the setup only (in our setup is $M_t \approx 1$ and $M_l \approx 10$). The sample dynamics enters via the number of dynamical modes $M_{dyn}(t_e)$ which depends on both the exposure time and the correlation time t_0 of the sample itself with $M_{dyn}(t_e) = 1$ for $t_0 \gg t_e$ (i.e. static sample) and $M_{dyn}(t_e) \gg 1$ for $t_0 \ll t_e$ (i.e. too fast for detection). The overall number of modes is related to the speckle contrast via $\beta(t_e) = \frac{1}{M(t_e)}$ and can be determined from a speckle image with the help of the ratio R of photon probabilities

$$R_{k,k+1}(t_e) = P(k, t_e)/P(k+1, t_e) \quad \text{Eq. (5)}$$

and the NBD as

$$M(t_e) = \frac{(1+k-R_{k,k+1}(t_e))\bar{k}}{R_{k,k+1}(t_e)\bar{k}-(1+k)} \quad \text{Eq. (6)}$$

which becomes particularly simple for $k = 0$ with $M(t_e) = \frac{\bar{k}}{R_{0,1}(t_e)\bar{k}-1}$. Thus the ratio of zero vs. one photon events allows to deduce the speckle contrast via

$$\beta(t_e) = R_{0,1}(t_e) - 1/\bar{k} \quad \text{Eq. (7)}$$

and we finally find the master formula for low intensity speckle visibility spectroscopy

$$R_{0,1}(t_e) - \frac{1}{\bar{k}} = \frac{\beta_0}{t_e} \int_0^{t_e} 2 \left(1 - \frac{t}{t_e}\right) |f(Q, \tau)|^2 d\tau. \quad \text{Eq. (8)}$$

Experiment

The experiment has been performed at the P10 coherence application beamline at PETRA III at DESY. A photon energy of 13 keV has been used with a beam size of $6 \times 3 \mu\text{m}^2$. A fast shutter produced the X-ray pulses with durations between 75 ms and 1000 ms. Temperatures of $T=190 - 235 \text{ K}$ around the glass transition have been achieved by a liquid nitrogen cryostat. The EIGER 4M detector[20] with a pixel size of $75 \times 75 \mu\text{m}^2$ and an active area of 2167×2070 pixels has been used. For reducing beam damage, we systematically scanned the sample through the X-ray beam by steps of $10 \mu\text{m}$ taking a single exposure for each exposure time t_e and sample position. Exposure times varied between 75 ms and 1000 ms.

We used the ionic liquid 1-octyl-3-methylimidazolium chloride ($\text{C}_{12}\text{H}_{23}\text{ClN}_2$). The mass absorption coefficient of the IL sample at 13 keV photon energy is $5 \text{ cm}^2/\text{g}$. The sample was filled into 1 mm quartz glass capillaries and sealed with epoxy resin. Calorimetric studies have shown that the glass transition of the sample is $T_G = 214\text{K}$ [21].

Results

Averaging 1000 diffraction patterns with 1 s exposure each yields the well-known pre-peak in the structure factor of ionic liquids with the maximum of the correlation located at $Q=2.8 \text{ nm}^{-1}$ (Fig. 1a). In crystallography the intensities and widths of Bragg peaks are sensitive markers of the loss of order due to beam damage helping to monitor even tiny radiation induced structural changes [22]. The situation is different for disordered samples such as liquids and glasses with no long-range order present, providing only broad diffraction features. In addition, the amount and sensitivity of beam damage depends on the chemical environment. For example, water solutions are very difficult due to the hydrolysis of water [23]. Nevertheless, often radiation damage manifests itself by more or less abrupt changes to the scattering intensities as for example observed for SAXS experiments from protein solutions [24].

In the same philosophy, we monitor here the scattering intensity from a single spot on the sample as a function of exposure time. We continuously exposed the sample on a fixed spot and acquired frames with an exposure time of 75 ms at a temperature of $T=205\text{K}$, i.e. below the glass transition temperature. Using the measured X-ray flux and calculated absorption properties of the ionic liquid we can convert the exposure time into the corresponding X-ray dose. Integrating the scattering signal over the Q -range indicated in Fig. 1a yields the scattering power as a function of absorbed X-ray dose (Fig. 1b). A loss in diffraction intensity of the nanoscale structure is detected starting at a dose of 50 kGy. The dose at which the intensity decreases by a factor of two is 220 kGy at a resolution of 2.1 nm yielding a dose-resolution of $10 \text{ kGy}/\text{\AA}$ which is three orders of magnitude smaller than the crystallography based dose-resolution of $10 \text{ MGy}/\text{\AA}$ of cryogenically cooled protein crystals suggested by Howells [22].

In our experiment, we used doses ranging from 640 Gy to a maximum value of 8.5 kGy. This maximum value corresponds to a dose-resolution of $0.4 \text{ kGy}/\text{\AA}$, at which no changes to the diffraction peak are visible. However, dynamic properties may be affected at doses below the threshold of structural damage [8]. In case the absorbed X-ray dose would be converted completely into local heating of the IL sample we calculate a maximum temperature rise of 1K

for an exposure time of 1 s. A standard XPCS experiment with 1000 images and 1 s exposure would have yielded doses larger than 15 MGy and therefore deep in the beam damage regime.

The dynamics of the sample can be inferred from the change of the photon probabilities as a function of exposure time t_e . There are two contributions to the change of photon probabilities in X-ray speckle visibility: the first one is the trivial scaling of the average intensity per pixel $\bar{k} = r \cdot t_e$ with r denoting the photon rate. The second factor is the change in mode number $M(t_e)$ which is associated with the dynamics of the sample. In Fig. 2 we plot the difference between the measured zero (blue) and one photon-probabilities (red) and the calculated ones with the simple scaling of the average intensity only for $T=200\text{K}$. Both curves in Fig. 2 deviate from zero and change with t_e indicating that the number of modes $M(t_e)$ is changing during the exposure. Specifically, we note that the number of detected 0-photon events is decreasing with increasing exposure time and the number of 1-photon events is increasing in agreement with an increasing mode number due to the dynamics of the sample. We observe a similar behavior for the 2- and 3- photon events.

To determine the correlation function, we calculate the ratio of the 0-, and 1-photon events and the averaged photon probability \bar{k} for all speckle images using the scattering signal within the area marked by the red lines in Fig. 1. From these values, we can obtain the speckle contrast β using Eq. (7). This contrast value is calculated for the 1000 recorded images for each exposure time t_e and for each temperature T . Two examples for the contrast β_{01} calculated from the ratio of 0- and 1-photon events for temperatures of $T=220\text{ K}$ and 200 K are shown in Fig. 3. Both contrasts drop as a function of exposure time with the 200 K data providing a much slower loss of speckle visibility indicating slower dynamics at lower temperatures. The correlation function at $T=220\text{ K}$ approaches a contrast value of zero at large values of the exposure time indicating that the speckle patterns are fully decorrelated at exposure times beyond 1 s. At lower temperatures, however, the dynamics is partially frozen on the time scales of seconds and beyond as the correlation functions do not approach the value of zero. It is also apparent that there are several relaxation mechanisms involved in the low temperature dynamics of the ionic liquid. At $T=200\text{ K}$ for example, in the glassy phase, we observe a fast relaxation with time scales below 100 ms, a second relaxation with time scales of 400 ms and a frozen-in component. We label the three observed processes by P1, P2 and P3 and the solid lines shown in Fig. 3 represents fits using an exponential function and a Kohlrausch-Williams-Watts (KWW) exponent of 0.7 for all three processes [25]. Unfortunately, the limited time window prevents a self-consistent refinement of the three different processes over the whole temperature range. We note, however, that multiple relaxation mechanisms have also been observed in the picosecond to nanosecond regime in the liquid phase at temperatures well above T_G [15].

The complete picture of nanoscale dynamics at the glass transition can be inferred from Fig. 4a showing the speckle contrast over the whole measured temperature interval around T_G . The appearance of a frozen-in component is apparent for time scales of 1000 ms and at temperatures of 210 K and below (see also contour plot Fig. 4b). This is where the system falls out of equilibrium and the slowest relaxation gets arrested. This relaxation is attributed to an overall (alpha) type relaxation of the nanoscale order in the IL [26]. However, we still observe dynamics on time scales of 100 - 200 ms in the glassy phase. As this motion does not fully decorrelate the speckle contrast it must be local in nature. However, the fact that it still contributes a rather large component to the decorrelation of the dynamic structure factor at

T_G indicates that the associated motion has a considerable spatial extension. The microscopic origin of this mode is not clear but one can relate it to the delicate balance of electrostatic and van-der Waals interactions from the ions and alkyl chains in the IL. This still allows for relaxation mechanisms on the nanoscale which do not freeze out completely below T_G . It is tempting to associate the observed increasing nanoscale order below T_G with the presence of this fast motion.

The speckle contrast at the largest available delay time of 1 s is a measure of the arrested component P3 of the dynamics. The temperature dependence of this component is plotted in Fig. 5(a) showing a sudden increase at a temperature which we associate with the glass transition. The maximum value of the non-ergodicity parameter is $f_c = 0.17$ at 200K (Fig. 5a). Connecting this to the Debye-Waller factor via $f_c = \exp(-Q^2\langle u^2 \rangle/3)$ we obtain an estimate for the localization length characterizing the range of motion associated with this fast mode. We find a value of $\sqrt{\langle u^2 \rangle} \approx 0.85$ nm which is smaller than the nanostructure correlation length of $L_{cor} \approx \frac{2\pi}{Q} = 2.4$ nm. In fact, this value is closer to typical charge alternation correlation lengths in the IL structure which appear at distances between 0.6 and 0.9 nm. Thus, this fast motion would be in the charge alternation domains and not be related to the apolar domains.

As we cannot disentangle the three processes over the whole temperature range we chose a different way to obtain further insight into the origin of the here observed dynamics. From the correlation functions, we evaluate an averaged relaxation time representing the mean decorrelation time for each temperature. The deduced time constants as a function of temperature are shown in Fig. 5b. Close to T_G we can disentangle frozen in and still active motions. The fast averaged motion show an activation energy of (25 ± 5) kJ/mol which is in the range of values reported for different relaxation processes in the liquid phase such as ionic diffusion processes, nanostructural relaxation, local reorientation of the alkyl chains and the imidazolium rings [26].

In conclusion, by spreading the dose over a large sample area and evaluating single photon events we demonstrate that XPCS experiment can be performed at X-ray doses several orders of magnitude smaller than previously. Using this method, we observe the nanoscale dynamics of an ionic liquid below the glass transition. The relaxation in the glassy phase is not completely frozen. Instead we find different processes which are still active in the glassy phase on times scales of 100 ms and below besides a frozen-in alpha type relaxation. This fast dynamic is associated with the peculiar nanostructure of the ionic liquids which still allows for motion below the calorimetric glass transition. It also becomes apparent that for a deeper understanding of the glass transition a larger range of time scales need to be probed which becomes available with the new diffraction limited storage rings (DLSR). Finally, we note that for example lysozyme proteins in solutions can tolerate doses of 400 Gy [24]. Therefore, our approach allows to tackle also the dynamics of biological macromolecules in solution at room temperatures [27].

Acknowledgements

This work is supported by the BMBF under project 05K13PS5 and the Swedish Research Council within the Röntgen-Angström-Cluster "Soft matter in motion". Parts of this research were carried out at PETRA III at DESY, a member of the Helmholtz Association.

References

- [1] J. Carnis *et al.*, *Sci Rep* **4**, 6017 (2014).
- [2] O. Shpyrko, *Journal of Synchrotron Radiation* **21**, 1057 (2014).
- [3] V. M. Giordano and B. Ruta, *Nature Communications* **7**, 10344 (2016).
- [4] B. Ruta, G. Baldi, Y. Chushkin, B. Rufflé, L. Cristofolini, A. Fontana, M. Zanatta, and F. Nazzani, *Nature Communications* **5** (2014).
- [5] B. Ruta, Y. Chushkin, G. Monaco, L. Cipelletti, E. Pineda, P. Bruna, V. M. Giordano, and M. Gonzalez-Silveira, *Phys Rev Lett* **109**, 165701 (2012).
- [6] M. Leitner, B. Sepiol, L.-M. Stadler, B. Pfau, and G. Vogl, *Nat Mater* **8**, 717 (2009).
- [7] G. Grübel and F. Zontone, *Journal of Alloys and Compounds* **362**, 3 (2004).
- [8] B. Ruta, F. Zontone, Y. Chushkin, G. Baldi, G. Pintori, G. Monaco, B. Rufflé, and W. Kob, *Scientific Reports* **7**, 3962 (2017).
- [9] M. Eriksson, J. F. van der Veen, and C. Quitmann, *Journal of Synchrotron Radiation* **21**, 837 (2014).
- [10] E. Weckert, *IUCrJ* **2**, 230 (2015).
- [11] P. Vodnala *et al.*, *AIP Conference Proceedings* **1741**, 050026 (2016).
- [12] C. DeCaro *et al.*, *Journal of Synchrotron Radiation* **20**, 332 (2013).
- [13] A. Triolo, O. Russina, H.-J. Bleif, and E. Di Cola, *The Journal of Physical Chemistry B* **111**, 4641 (2007).
- [14] R. Hayes, G. G. Warr, and R. Atkin, *Chem Rev* **115**, 6357 (2015).
- [15] M. Kofu, M. Nagao, T. Ueki, Y. Kitazawa, Y. Nakamura, S. Sawamura, M. Watanabe, and O. Yamamuro, *J Phys Chem B* **117**, 2773 (2013).
- [16] C. Gutt, L. M. Stadler, A. Duri, T. Autenrieth, O. Leupold, Y. Chushkin, and G. Grubel, *Opt Express* **17**, 55 (2009).
- [17] G. Grübel, G. B. Stephenson, C. Gutt, H. Sinn, and T. Tschentscher, *Nucl Instrum Meth B* **262**, 357 (2007).
- [18] R. Bandyopadhyay, A. S. Gittings, S. S. Suh, P. K. Dixon, and D. J. Durian, *Review of Scientific Instruments* **76**, 93110 (2005).
- [19] W. G. Joseph, *Speckle phenomena in optics: theory and applications* (2007).
- [20] I. Johnson *et al.*, *Journal of Instrumentation* **9**, C05032 (2014).
- [21] O. Yamamuro and M. Kofu, *IOP Conference Series: Materials Science and Engineering* **196**, 12001 (2017).
- [22] M. R. Howells *et al.*, *J Electron Spectros Relat Phenomena* **170**, 4 (2009).
- [23] W. M. Garrison, *Chemical Reviews* **87**, 381 (1987).
- [24] S. Kuwamoto, S. Akiyama, and T. Fujisawa, *Journal of Synchrotron Radiation* **11**, 462 (2004).
- [25] A. Madsen, R. L. Leheny, H. Guo, M. Sprung, and O. Czakkel, *New Journal of Physics* **12**, 55001 (2010).
- [26] M. Kofu, M. Tyagi, Y. Inamura, K. Miyazaki, and O. Yamamuro, *The Journal of Chemical Physics* **143**, 234502 (2015).
- [27] V. Preeti *et al.*, *aip*, 50026 (2016).

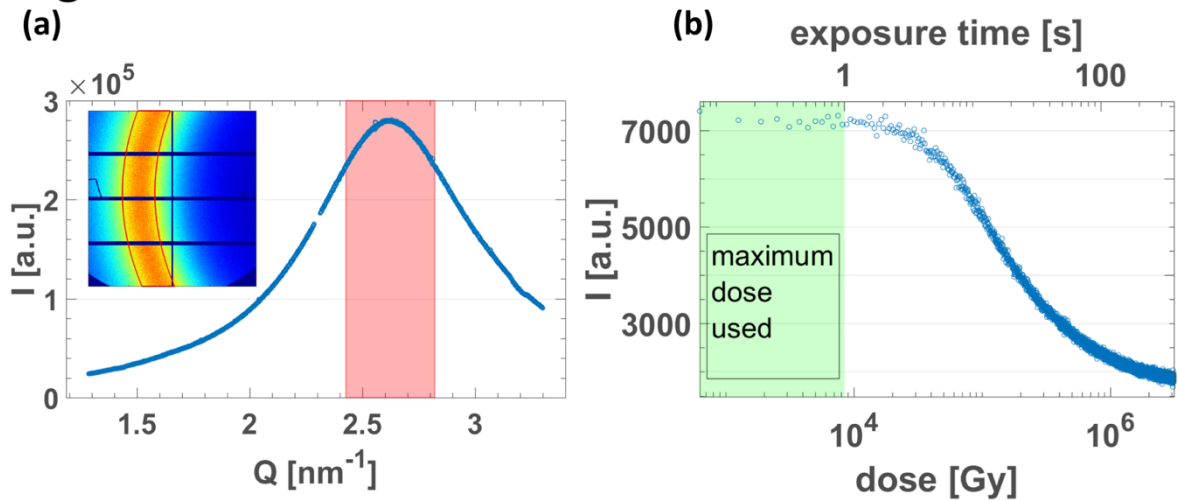
Fig.1

Fig.1:(a) X-ray diffraction pattern from the supercooled ionic liquid C8mimCl associated with the nanoscale order. The inset shows the diffraction pattern as recorded on the area detector. The red box indicates the Q -range used for the XPCS analysis. (b) The integrated X-ray signal from the area of the red box in (a) plotted as a function of the absorbed X-ray dose/exposure time. The green area indicates the range of doses used in the experiment.

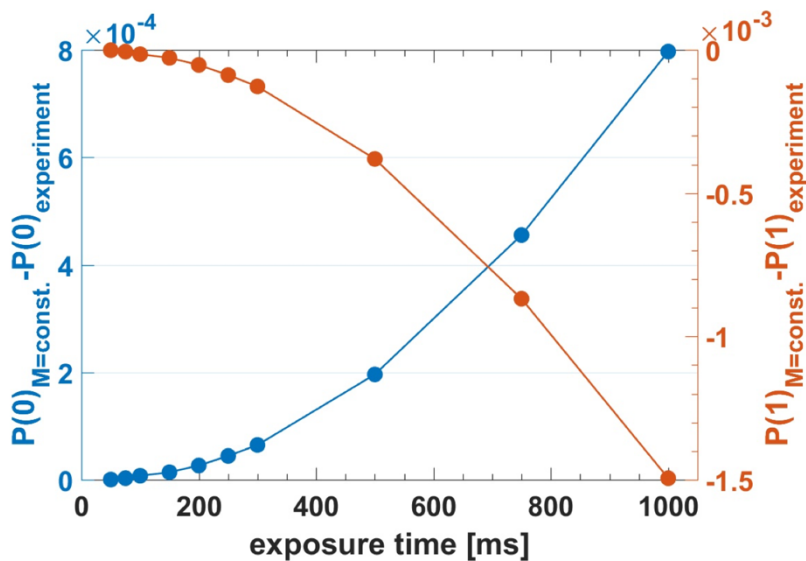
Fig.2

Fig. 2: Blue data: The difference between the actual measured 0-photon probability and the 0-photon probability calculated assuming no dynamics but a simple increase of the mean count rate according to $\bar{k} = r \cdot t_e$. The decreasing number of 0-photon events indicates the decreasing speckle contrast as a function of exposure time caused by the sample dynamics. Red data: same plot as in blue but here for the 1-photon probabilities.

Fig.3

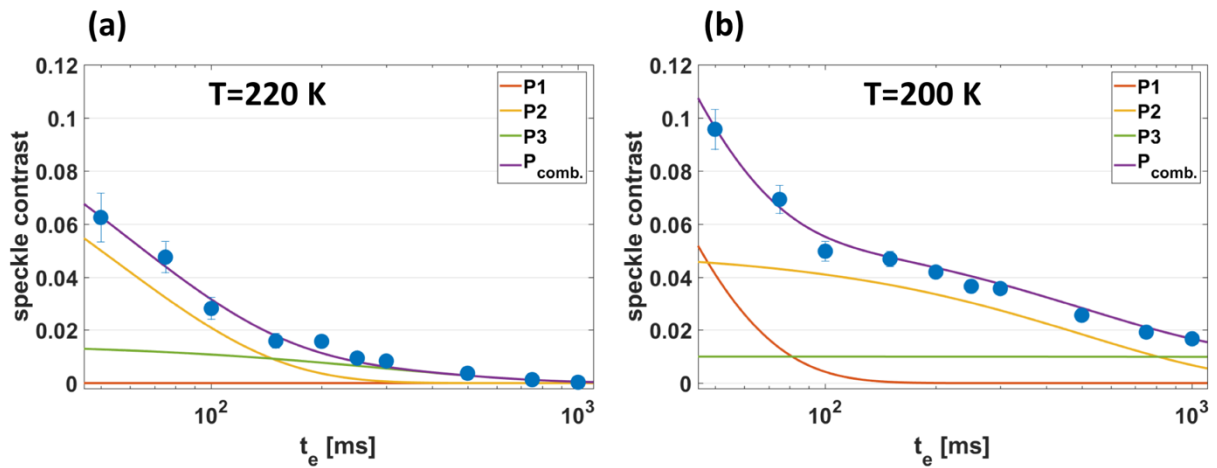


Fig.3: Speckle contrast of the ionic liquid as a function of exposure time for temperatures of 220K and 200K and $Q=2.6\text{nm}^{-1}$, respectively. The solid lines are assignments to three different processes labeled P1, P2 and P3. The calorimetric glass transition temperature is 214K.

Fig.4

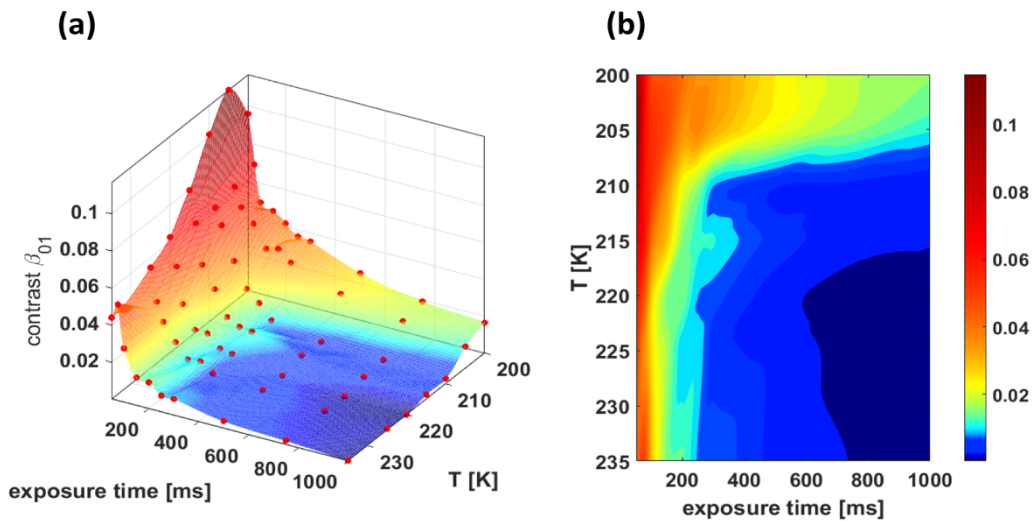


Fig.4: (a) Speckle contrast as a function of temperature and delay time for the ionic liquid C8mimCl at $Q=2.6\text{nm}^{-1}$. The dynamics is progressively slowing down upon approaching T_G with a separation in a fast and slow frozen-in dynamics visible at the lowest temperatures. (b) Contour plot of the pattern shown in (a).

Fig.5

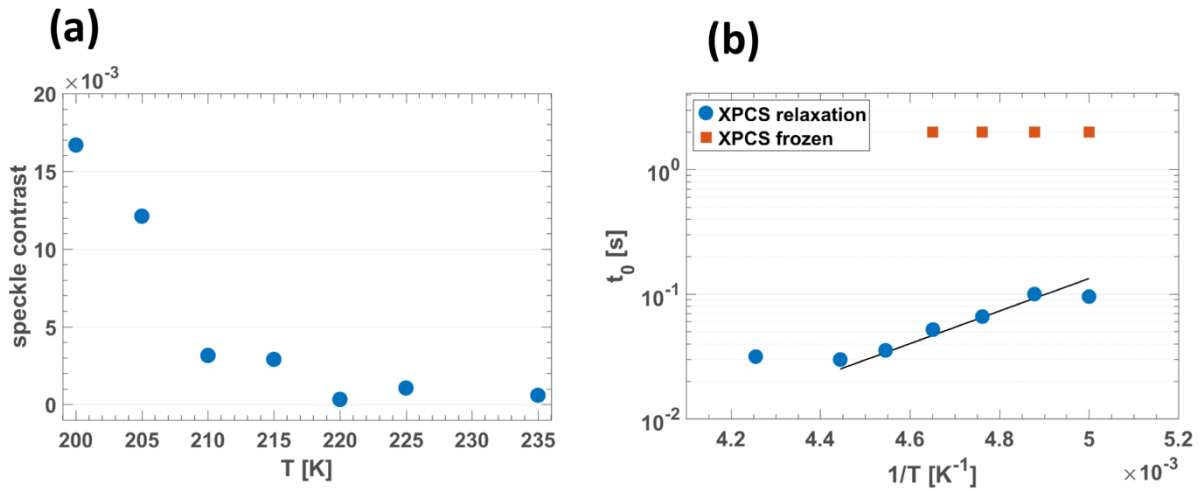


Fig. 5: (a) The X-ray speckle contrast at $t_e = 1s$ exposure time as a function of temperature. (b) Temperature dependence of the deduced time constants in the IL resulting from fitting the curves shown in Fig. 4(a) with Eq. (8). The blue dots represent an averaged relaxation time and the red squares the appearance of the frozen in components (i.e. dynamics slower than 1s). The black line represents an Arrhenius fit with an activation energy of 25 kJ/mol.